International Journal of Pharmaceutics 388 (2010) 151–158

Contents lists available at ScienceDirect

International Journal of Pharmaceutics

journal homepage: www.elsevier.com/locate/ijpharm

Microencapsulation of self-microemulsifying system: Improving solubility and permeability of furosemide

A. Zvonar, K. Berginc, A. Kristl, M. Gašperlin*

Faculty of Pharmacy, University of Ljubljana, Aškerčeva 7, 1000 Ljubljana, Slovenia

ARTICLE INFO

Article history:
Received 14 October 2009
Received in revised form
18 December 2009
Accepted 24 December 2009
Available online 7 January 2010

Keywords:
Microcapsules
Self-microemulsifying systems
Vibrating nozzle
Furosemide
Drug release
Permeability

ABSTRACT

The primary goal of this study was to formulate Ca-pectinate microcapsules with self-microemulsifying core to enhance the solubility and permeability of BCS class IV drug furosemide. An Inotech IE-50R encapsulator equipped with a concentric nozzle was utilized to transform liquid self-microemulsifying system (SMES) to solid microcapsules. Self-microemulsifying core was optimized with respect to drug loading capacity and encapsulation efficiency and evaluated for its impact on furosemide permeability through rat small intestine and Caco-2 cell monolayers. Retention of the core phase was considerably improved (up to 70–80%) by optimization of the SMES and microcapsules' drying process. Incorporation of furosemide in self-microemulsifying core of microcapsules resulted in improved permeability and drug release characteristics in comparison to microspheres (without SMES in the core). The obtained results illustrate the prospective use of microcapsules with self-microemulsifying core for the delivery of compounds with poor biopharmaceutical properties via the oral route.

1. Introduction

Oral delivery is the preferred route for drug administration. However, for many active pharmaceutical ingredients it remains a serious challenge due to limited oral bioavailability, high intra- and inter-subject variability, and lack of dose proportionality. Development of adequate pharmaceutical formulation is the valuable key step for improving poor water solubility and/or poor membrane permeability that are responsible for the low fraction of the drug dose absorbed. According to the literature data, there is a growing interest in the lipid- and surfactant-based systems e.g. lipid solution, surfactant dispersion emulsion, liposomes, microemulsion, dry emulsion and self-(micro)emulsifying formulations (Shah et al., 1994; Burcham et al., 1997; Šentjurc et al., 1999; Jumaa et al., 2002; Neslihan and Benita, 2004; Porter et al., 2007; Patil et al., 2007).

SMES are mixtures of oil, surfactant and hydrophilic co-surfactant capable of forming fine o/w (micro)emulsion during the gentle agitation provided by the digestive motility of the stomach and intestine (Shah et al., 1994; Constantinides, 1995). The spontaneous formation of a (micro)emulsion on SMES dilution with intestinal fluids advantageously delivers the drug in its dissolved form throughout its transit through the gastrointestinal tract, thus avoiding a drug dissolution step and providing a large interfacial surface area for drug absorption (Pouton, 2000; Porter et al., 2007). Apart from solubilisation, the presence of lipids and surfactants in the formulation provides satisfactory environment for the improvement of the bioavailability. Eventually, inhibition of P-glycoprotein-mediated drug efflux and first-pass gut metabolism (cytochrome enzymes), increased GIT membrane permeability and increased lymphatic transport direct to the systemic circulation are well recognized mechanisms by which the formulation constituents (i.e. lipids, surfactants) improve intestinal absorption (Pouton, 2000; Rege et al., 2002; Wandel et al., 2003; Constantinides and Wasan, 2007; Porter et al., 2007).

In attempts to combine the advantages of SMES with those of solid dosage forms and overcome the shortcomings of liquid formulations, increasing attention has been focused on solid self-(micro)emulsifying formulations in recent years (Jannin et al., 2007). SMES are usually filled in soft gelatin capsules, but they can also be transformed into granules, pellets, powders for dry filled capsules or tablet preparations (Nazzal and Khan, 2006; Serratoni et al., 2007; Abdalla et al., 2008; Tan et al., 2009). In our previous study an innovative approach of incorporating SMES into Ca-alginate microcapsules by using vibrating nozzle method has been reported (Homar et al., 2007). However, this initially developed method has not been sufficiently optimized in order to enable repeatable production of microcapsules with high encapsulation efficiency.

* Corresponding author. Tel.: +386 1 47 69 634; fax: +386 1 42 58 031.
E-mail address: mirjana.gasperlin@ffa.uni-lj.si (M. Gašperlin).

0378-5173/$ – see front matter © 2010 Elsevier B.V. All rights reserved.
doi:10.1016/j.ijpharm.2009.12.055

The main scope of the current study was therefore to originate microcapsules with Ca-pectinate shell and furosemide-loaded SMES as the core phase. This versatile SMES formulation would be potential approach for enhancing low permeability and solubility of a model drug furosemide, which are the two critical factors responsible for its poor and highly variable human bioavailability (Lee and Chiou, 1983; Chiou and Barve, 1998). Moreover, optimization of self-microemulsitying core in order to enhance drug loading capacity and encapsulation efficiency was principal novelty regarding to the initial approach developed by our research group. To confirm improved permeability by implementing furosemide into SMES, tests on rat small intestine and on Caco-2 cell monolayers have been evaluated. Additionally, the influence of core composition on drug release profile from dried microcapsules was examined.

2. Materials and methods

2.1. Materials

SMES was composed of the medium chain triglyceride Mygliol 812® (Hüls, Germany) as lipophilic phase, caprylocaproyl macrogolglycerides Labrasol® (Gattefosse, France) as surfactant and polyglyceryl-6 dioleate Plurol Oleique® (Gattefosse, France) as co-surfactant. Pectin (Genu® pectin type LM-104 AS-Z) was used as polymer matrix (CP Kelco, Denmark) and chitosan (Chitosan, low viscosity) as coating polymer (Fluka, Germany). Furosemide, and lactose (mesh 200) as shell phase additive, were kindly provided by Lek Pharmaceuticals d.d.. White wax (Lex d.d., Slovenia) and colloidal silica (Aerosil 200, Degussa, Dusseldolf, Germany) were used as the SMES thickening agents. Fluorescein sodium (Flu), rhodamine 123 (Rho), furosemide, verapamil (Ver), benzbromarone (BB) and salts for incubation salines were from Sigma–Aldrich Chemie (Deisenhofen, Germany). All chemicals used in this study were of analytical grade.

2.2. Methods

2.2.1. Preparation of SMES

SMES was prepared by blending the Labrasol® and Plurol oleique® in a 4:1 mass ratio to obtain the surfactant mixture. The ratio was determined by Špiclin et al. (2003). Mygliol 812® was then added in different mass concentrations (10, 12, 20, 30%, w/w) and mixed to give a homogeneous mixture. The optimal system was then mixed for 24 h at room temperature with different amounts of $CaCl_2$ (0.02–0.5%, w/w) and thickened with white wax or colloidal silica (2, 4 or 6%, w/w). Drug loaded SMES were prepared by adding furosemide at 1 and 5 (completely solubilised drug) or 10 (partly suspended drug) % (w/w) concentration prior thickening.

2.2.2. Determination of solubilization capacity

The saturated solubility of furosemide in the SMES of different compositions was determined by adding an excess of drug and stirring continuously for at least 72 h at ambient temperature to reach equilibrium. The supernatant was filtered with a 0.45 μm membrane filter and analyzed by HPLC after appropriate dilution with a mixture (80:20, v/v) of acetonitrile and bidistilled water.

2.2.3. In vitro transport studies across Caco-2 cell monolayers

Caco-2 cells were obtained from the American Tissue Culture Collection (ATCC) HTB.37, lot 2463681. Cell monolayers were grown on Snapwell Costar culture inserts with a polycarbonate membrane (diameter 12 mm and pore size 0.4 μm). 100,000 cells/filter membrane was used for seeding and the medium was changed every two days. At day 15, transepithelial electrical resistance (TEER) was measured for each filter with Caco-2 cell monolayers. If the TEER values were in the range of 450–750 Ω cm^2, the Caco-2 cell monolayers were used for the subsequent testing of permeability at day 21.

The inserts with Caco-2 cells were carefully rinsed with Ringer buffer and placed between two compartments of EasyMount side-by-side diffusion chambers (Physiologic Instruments, San Diego, USA). 2.5 ml of bathing solution (Ringer buffer) on each side of the Caco-2 cell monolayer was maintained at 37 °C and continuously oxygenated and circulated by bubbling with carbogen (95% O_2, 5% CO_2). 10 mM glucose and 10 mM mannitol were always added to the basolateral (BL) and apical (AP) sides, respectively. The apical solution contained, in addition, 0.2% (v/v) of SMES when the influence of this lipid vehicle on passive and active transport processes was evaluated. The concentration of 0.2% (v/v) SMES was chosen as the usual SMES amount contained in soft gelatine capsules, and calculated to 250 ml of water/Ringer buffer. After 25 min of preincubation, 0.5 ml of the concentrated solution containing investigated substance (FLU, Rho123 or furosemide) was added to the AP side (if studying apical-to-basolateral (AP-BL) transport) or to the BL side (if studying basolateral-to-apical (BL-AP) transport). 250 μL samples were withdrawn from the acceptor side every 20 min and replaced each time by fresh Ringer buffer containing all necessary ingredients at appropriate concentrations. The specific inhibitors of Pgp and MRP-2 used in the experiments were verapamil and benzbromarone. They were added to the apical solution to give final concentrations of 200 and 50 μM, respectively. Only those Caco-2 cell monolayers with TEER values that remained constant during the whole experiment were used.

2.2.4. In vitro transport studies across rat small intestine

Experiments conformed to the Law for the Protection of Animals (Republic of Slovenia) and were registered at the Veterinary Administration of the Republic of Slovenia. They were performed in the manner described previously (Berginc et al., 2007). Rat small intestine was obtained from male Wistar rats (250–320 g) fasted 18 h prior to the experiments. After euthanasia and laparotomy, the intestine was rinsed with ice-cold 10 mM glucose Ringer solution. The experimental procedure was performed in the same manner as described in Section 2.2 for Caco-2 cell monolayers.

2.2.5. Electrical measurements

The diffusion chambers were equipped with two pairs of Ag/AgCl electrodes for measuring transepithelial potential difference (PD) and short circuit current (Isc) with a multichannel voltage–current clamp (model VCC MC6, Physiologic Instruments). The viability and integrity of tissue and Caco-2 cells were checked by monitoring PD, Isc and TEER every 20 min during the experiments. In viable rat tissues and Caco-2 cells, TEER did not change significantly during the experiment. The average TEER was calculated and also used for evaluating the tissue/cell integrity and viability. The viability of rat small intestine was additionally checked by recording the increase of Isc and PD after the addition of stock glucose solution to the mucosal compartment at the end of experiment (final glucose concentration was 25 mM). Tissue segments were considered viable if the PD value after the addition of glucose was lower than −1.0 mV and if the average TEER values recorded during the experiment were between 20 and 40 Ω cm^2. The Caco-2 cell culture monolayers were considered viable if the average TEER values between 15 and 150 or 225 min were in the range of 500 and 800 Ω cm^2, and if they exhibited a PD lower than −0.5 mV during the experiment.

2.2.6. FLU and Rho123 detection, HPLC parameters

Concentrations of FLU and Rho123 were measured with a fluorescence detector Tecan GENious (λ_{ex} = 485 nm, λ_{em} = 535 nm). 50 μL of a sample was diluted with 100 μL of 0.025 M NaOH to

measure the concentration of FLU and with 100 μL of 0.01 M HCl for Rho123.

The quantity of furosemide in the samples was determined by HPLC analysis using a Gemini C-18 column (5 μm, 300 mm × 3.9 mm; BIA Separations d.o.o., Slovenia). The mobile phase, which consisted of acetonitrile, phosphate buffer (pH 4.0, 0.01 M) and methanol (45:45:10, v/v/v), was used at a constant flow rate of 1.4 ml/min. The UV detector was set to 238 nm. The lower limit of quantification was 0.223 μg/ml and the response was linear from 0.223 to 262 μg/ml. An external standard was used in all cases to determine the concentration of furosemide.

2.2.7. Data analysis

The apparent permeability coefficient (P_{app}) was calculated according to Eq. (1):

$$P_{app} = \frac{dc}{dt}\frac{V}{c_0 A} \quad (1)$$

where dc/dt is the change in concentration of the examined substance in the acceptor compartment per unit time under steady state conditions, V is the volume of the acceptor compartment, A is the exposed surface area (1 cm^2 for rat jejunum and 1.13 cm^2 for Caco-2 cell monolayers) and c_0 is the initial concentration of the examined substance in the donor solution.

Results are presented as means ± SD of at least three measurements. Data were evaluated statistically using SPSS 16.0 for Windows. Where appropriate, F-test for testing the equality of variances and, afterwards, 2-tailed Student's t-test ($\alpha = 0.05$), were used.

2.2.8. Density measurement

Densities were determined with a Density Meter—DMA 5000 (Anton Paar, Austria) at 20 ± 0.009 °C. The accuracy of density measurements was within $\pm 5 \times 10^{-6}$ kg dm^{-3}.

2.2.9. Preparation of microcapsules

Microcapsules with a self-microemulsifying core were prepared by a vibrating nozzle method using an Inotech IE-50R encapsulator (Inotech, Switzerland) equipped with a 500/750 μm concentric nozzle, a 60 ml syringe containing the shell forming phase (2%, w/w, water solution of pectin containing 5%, w/w, lactose) and an air-pressure solution delivery system containing the core phase (Fig. 1). The vibration frequency of the membrane used to break up the liquid jet was set at 3000 Hz and the amplitude at 3. An additional electrostatic field of 0.9 kV was applied between the nozzle and the hardening solution, thus preventing potential coalescence of formed beads during the flight or in approaching the surface of the gelation solution. For complete gel hardening, microcapsules were incubated in 0.5 M $CaCl_2$ solution for 15 min. To reinforce the microcapsules' shell, chitosan coating was additionally applied by incubating the microcapsules in an 1% acetic acid solution of chitosan (1 mg/ml) for 5 min. Afterwards microcapsules were rinsed with water and dried according to different procedures (in air at the room temperature, in vacuum, by freeze-drying (Beta 1-8K, Christ, Germany), or in a fluid bed system (Strea 1, Niro Aeromatic, Switzerland).

Reference microspheres (without SMES in the core) were prepared from the shell phase loaded with 1 or 10% (w/w) of furosemide, following the same procedure.

2.2.10. Encapsulation efficiency

The efficiency of furosemide encapsulation in microcapsules was determined directly in freshly produced and in dried microcapsules. The furosemide-loaded microcapsules ($n = 15$) were crushed and soaked in beakers filled with 50 ml of distilled water and ethanol mixture (50:50, v/v) for at least 12 h. Samples were then filtered through the 0.45 μm membrane filter and analyzed by HPLC. The mean encapsulation efficiency of three replicate experiments, calculated according to Eq. (2) for cross-linked (undried) and Eq. (3) for dried microcapsules is reported:

$$\text{encapsulation efficiency 1 (\%, w/w)} = \frac{\text{mass of drug in crosslinked microcapsules} \times 100}{\text{mass of drug in non-crosslinked microcapsules}} \quad (2)$$

$$\text{encapsulation efficiency 2 (\%, w/w)} = \frac{\text{mass of drug in dried microcapsules} \times 100}{\text{mass of drug in non-crosslinked microcapsules}} \quad (3)$$

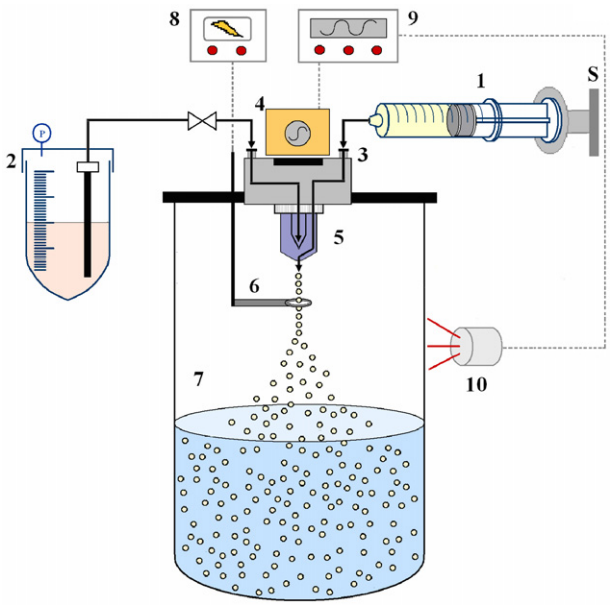

Fig. 1. A schematic representation of the microcapsule production process. (1) Syringe with shell forming phase. (2) Delivery bottle with core forming phase (SMES). (3) Pulsation chamber. (4) Vibration system. (5) Concentric nozzle. (6) Electrode. (7) Reaction vessel with hardening solution. (8) Electrostatic charge generator. (9) Frequency generator. (10) Stroboscope. P, pressure control system; S, syringe pump.

2.2.11. Optical analysis of microcapsules

The size, shape and surface morphology of dried microcapsules were observed under an Olympus SZX 12 optical microscope mounted with a digital camera (3CCD Color Video Camera, Power HAD, Sony, Japan).

2.2.12. In vitro dissolution test

Drug release was studied using the USP apparatus 2 (VK7000, VanKel, USA). The dissolution medium was 900 ml of either pH 3 hydrochloric acid aqueous solution or pH 6.8 phosphate buffer, both at 37 ± 0.5 °C and stirred at 75 rpm. At the predetermined intervals (hours) 10 ml sample aliquots were withdrawn, filtered through a 0.45 μm membrane filter and assayed by HPLC method. Cumulative percentages of the drug dissolved from the products were calculated and plotted vs. time.

3. Results and discussion

3.1. Determination of optimal SMES composition

The qualitative composition of SMES was selected on the basis of our previous work (Špiclin et al., 2003; Homar et al., 2007). SMES with different oil phase/surfactant ratios were tested to obtain

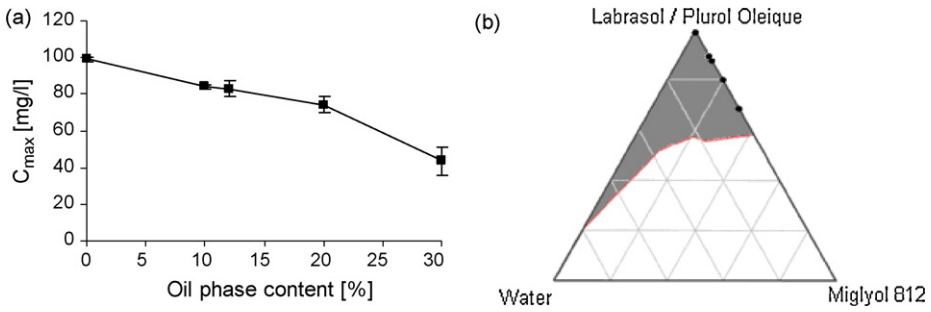

Fig. 2. (a) Furosemide loading capacity of SMES (c_{max}) as a function of oil phase content in SMES and (b) phase diagram of the system containing (Labrasol®:Plurol oleique® = 4:1)/Miglyol 812®/water; dark area—microemulsions, white area—unstable emulsions (mixtures investigated for loading capacity are marked with black dots).

the composition having the highest furosemide loading capacity (Fig. 2a). The greatest solubilization of furosemide (~100 mg/ml) was achieved in the pure surfactants mixture. Addition of oil decreased the solubilization capacity until it reached a value of approximately 59 mg/ml at 30% (w/w) oil phase. Besides solubilization capacity the area of the self-microemulsifying region in the phase diagram was taken into consideration in order to select a suitable self-microemulsifying formulation (Fig. 2b). On the basis of these results, SMES with 12% (w/w) oil phase content was selected as core phase for the production of microcapsules, due to the largest area where microemulsions are formed upon dilution and high solubilization capacity (~86 mg/ml). After dilution of selected SMES with 1 mM hydrochloric acid solution (0.5 ml SMES/250 ml) the solubility of furosemide (5.31 mg/ml) was still 212-fold higher than its solubility in water (0.025 mg/ml) (Beyers et al., 2000). Previously the internal structures of the systems formed on dilution of SMES with aqueous phase have been determined and their stability confirmed (Zvonar et al., 2009).

3.2. *Influence of SMES on furosemide permeability through rat small intestine and Caco-2 cell monolayers*

The furosemide and fluorescein permeabilities were evaluated through different parts of the rat small intestine (duodenum, jejunum, and ileum) and through Caco-2 cell monolayers. The permeabilities of furosemide alone in all segments of the rat small intestine and Caco-2 cell monolayers did not exceed the limits of 10×10^{-6} and 1×10^{-6} cm/s, respectively. This low permeability is usually exceeded with high permeable compounds, according to previous experiments in our laboratory with low (atenolol, 4.4×10^{-6} cm/s) and high (propranolol, 29.5×10^{-6} cm/s) permeability standards. The intestinal permeability of furosemide decreased along the small intestine, the duodenum being significantly ($\alpha < 0.05$) more permeable than the ileum. In the presence of 0.2% (v/v) SMES, significantly higher furosemide permeabilities were observed in all segments of the intestine and in Caco-2 cell monolayers compared to corresponding reference values (Fig. 3). The furosemide permeabilities determined in the duodenum and jejunum in the presence of SMES were significantly higher ($\alpha < 0.05$) than that measured with SMES in the ileum.

Oil-in-water microemulsions formed in the gastrointestinal fluids under mild agitation after SMES consumption enhance absorptive (M-S and AP-BL) permeability of low permeable compounds (Xianyi et al., 2005; Daham and Hoffman, 2007). Because of the close contact between the apical membrane and oil droplets of microemulsions the surfactants redistribute more readily from the oil droplets to the apical membrane. This creates polar membrane defects responsible for altered membrane fluidity (Xianyi et al., 2005; Daham and Hoffman, 2007), which favours the absorption of low permeable or otherwise nonabsorbable compounds; in our case furosemide. Furthermore, there is another mechanism, which could favour higher M-S/AP-BL permeability of furosemide, observed in this study. Namely, a SMES component often used—Labrasol®, has been investigated and shown, that in sufficiently high concentrations (i.e. 1%, w/v) it induces irreversible tight junction defects, which demonstrate themselves as significantly higher permeability of paracellular marker mannitol and 80% TEER decrease (Xianyi et al., 2005). However, because of irreversible changes of tight junction architecture (redistribution of ZO-1 proteins, changes of actin structure), the integrity and polarity of the Caco-2 cell monolayers could not be preserved at 1% (w/v) of Labrasol®. Since the concentration of SMES used in our study was only 0.2% (v/v), Labrasol® concentration was low enough not to hamper intestinal/Caco-2 cell vitality or integrity, which was assessed by measuring TEER values. The SMES presence did not cause any changes of TEER values compared to TEER values determined without SMES (data not shown), therefore tight junctions structure and function could not be altered. However, the permeability values of fluorescein, a paracellular permeability marker, used in this study to assess tight junction integrity, presented in Fig. 4, clearly indicate that in the presence of 0.2% (v/v) SMES, higher fluorescein permeabilities were observed through Caco-2 cell monolayers and through all intestinal segments but significant fluorescein permeability increase was observed only in the ileum and not in the other intestinal segments or Caco-2 cells. According to these data, Labrasol® could induce some minor reversible openings of tight junctions but most probably the main mechanism behind the increased fluorescein and furosemide permeabilities lies in the altered membrane fluidity and polar defects caused by surfactant Labrasol®. The structural membrane alterations in SMES

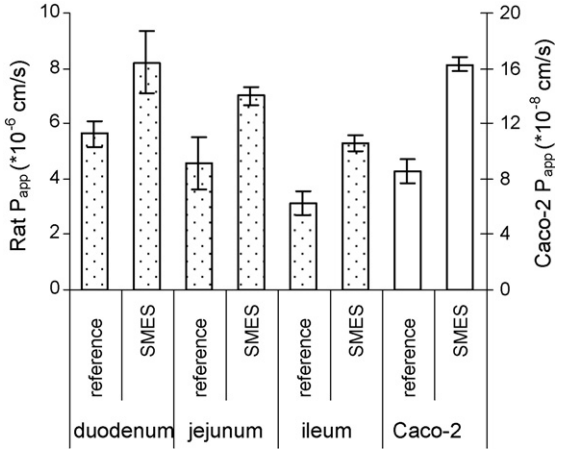

Fig. 3. M-S/AP-BL permeability of furosemide (100 μM) through the rat small intestine: duodenum, jejunum, ileum (presented in dotted bars) and Caco-2 cell monolayers (empty bars) alone (reference) and in the presence of 0.2% (v/v) of SMES. The data are presented as the average values and SEM of at least three measurements.

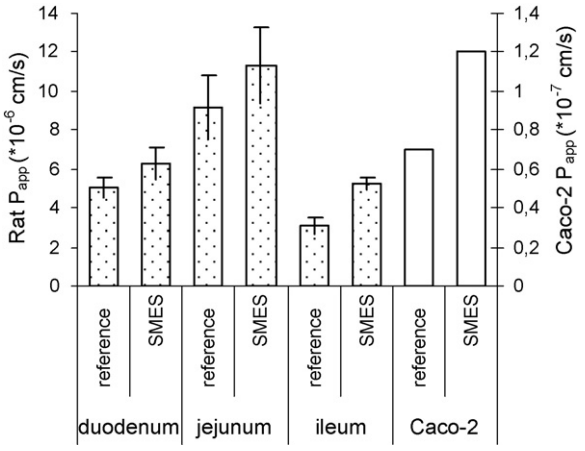

Fig. 4. M-S/AP-BL permeability of the paracellular marker fluorescein (10 μM) through the rat small intestine: duodenum, jejunum, ileum and Caco-2 cell monolayers alone (reference) or in the presence of 0.2% (v/v) of SMES in the mucosal/apical sides. The data are means and SEM of at least three measurements.

presence favour higher transcellular permeability of fluorescein and furosemide but at the same time the concentrations of SMES and Labrasol® used were in the range, where cell/tissue vitality and integrity were not affected.

Furosemide is also a substrate for intestinal and hepatic efflux transporters (Siissalo et al., 2009). The secretion of a low permeability drug that has just permeated through the apical membrane, leads to even lower absorption to the plasma and hence lower fraction of the dose absorbed. To evaluate the transport systems involved in intestinal furosemide secretion, we determined the S-M permeabilities of furosemide in rat duodenum and ileum (Table 1). It is known that in the proximal part of small intestine the most abundantly expressed transporters are MRP-2 (Maclean et al., 2008), which can be inhibited by benzbromarone. On the other hand, Pgp transporters, whose expression increases along the gastrointestinal tract (Maclean et al., 2008), can be inhibited by verapamil. In the duodenum, there was a significant decrease in S-M permeability after the addition of 50 μM benzbromarone. However, in the ileum, the S-M permeability of furosemide decreased after the addition of 200 μM verapamil, but the effect was not significant. One can therefore conclude that furosemide is most probably transported in the S-M direction mostly by MRP-2, whereas by Pgp transporters only partly. Similar observations were reported by Shawn et al. (1999), who noticed significantly reduced BL-AP furosemide permeabilities in the presence of MRP-2 inhibitor probenecid. Furthermore, the S-M/BL-AP furosemide permeabilities were also lower in the presence of mucosal/apical 0.2% (v/v) SMES in duodenum, ileum and in Caco-2 cell monolayers than in the reference experiments. This is in accordance with the findings of Daham and Hoffman (2007), who also observed inhibition of intestinal efflux transporters activity in the presence of lipid vehicles. Since the effect of SMES on S-M/BL-AP permeability of furosemide can most probably be ascribed to MRP-2 inhibition, additional experiments were performed to address the effect of SMES on Pgp transporters. These efflux transporters have namely very broad substrate specificity and consequently a strong impact on bioavailability. For this purpose rhodamine 123, a known Pgp substrate, was used. 0.2% (v/v) SMES significantly lowered S-M/BL-AP rhodamine 123 permeability, indicating that SMES is able to inhibit both intestinal efflux transporters.

3.3. Formulation of microcapsules with self-microemulsifying core

Liquid SMES was transformed into a solid formulation by microencapsulation into a Ca-pectinate matrix. The shell forming phase (pectin solution) envelopes the core phase (furosemide-loaded SMES) as they flow together through the concentric nozzle, forming a continuous jet that is broken apart into droplets by vibration of the membrane. When these droplets come in contact with hardening solution, a sol–gel transition of pectin in the shell occurs, encapsulating SMES with the drug in the core.

3.3.1. Optimization of self-microemulsifying core

The selected SMES was optimized, with respect to furosemide solubilisation capacity, for incorporation in Ca-pectinate microcapsules. The self-microemulsifying ability of the core phase is responsible for the majority of beneficial effects that we aimed to achieve. However, it is also responsible for mixing the core with the aqueous shell forming phase that starts immediately after they come into contact with each other. The direct consequence of this mixing is that the core leaks during the microcapsule production process, which decreases encapsulation efficiency. Therefore, the greatest challenge in the preparation of microcapsules with self-microemulsifying core is to reduce the undesirable mixing between the two phases.

Different excipients were added to the SMES to reduce core leaking and their influence on furosemide encapsulation was studied (Fig. 5). $CaCl_2$ was added to core phase in different amounts to promote shell hardening from the inside out as soon as the capsules were formed. The encapsulation of furosemide-loaded SMES increased from around 2 to 50% by increasing the content of $CaCl_2$ in the core phase from 0 to 0.5 mg/g SMES (Fig. 5). When $CaCl_2$ was added to SMES in higher amounts the microencapsulation process was disabled by clogging of the nozzle. A similar effect was observed previously (Homar et al., 2007).

Encapsulation was increased to a comparable level (up to 50%) by adding 2–6% (w/w) of thickening agents (colloidal silica or white wax) to SMES (Fig. 5); when the content of thickening agents was above 6% (w/w) the viscosity of the core phase was too high to enable production of microcapsules. The assumption was made that, besides the $CaCl_2$-promoted gelling at the core–shell interface, lowering of the process temperature could also decrease the mixing between the two phases. Encapsulation was considerably higher when the core phase was cooled to 5 °C (data not shown); this can be explained by decreased core–shell mixing due to cooling-induced increase in SMES viscosity. In order not to increase the

Table 1
The S-M/BL-AP permeability of furosemide (100 μM) and rhodamine 123 (20 μM) determined through the rat duodenum, ileum and Caco-2 cell monolayers alone (Ref), and in the presence of inhibitors added to the apical/mucosal side (200 μM verapamil—Ver, 50 μM benzbromarone—BB) or SMES 0.2% (v/v). The data are average values with standard deviations of at least three measurements.

P_{app} ($\times 10^{-6}$ cm/s)	Furosemide				Rhodamine 123	
	Ref	Ver	BB	SMES	Ref	SMES
Duodenum	16.7 ± 3.9	–	5.1 ± 0.5[a]	9.9 ± 3.8[a]		
Ileum	14.0 ± 3.8	9.4 ± 2.7	–	9.9 ± 4.6	24.3 ± 8.6	4.4 ± 1.3[a]
Caco-2	1.4 ± 0.0			1.0 ± 0.1[a]		

[a] Significant (Student's t-test, $\alpha = 0.05$) effect of inhibitors/SMES.

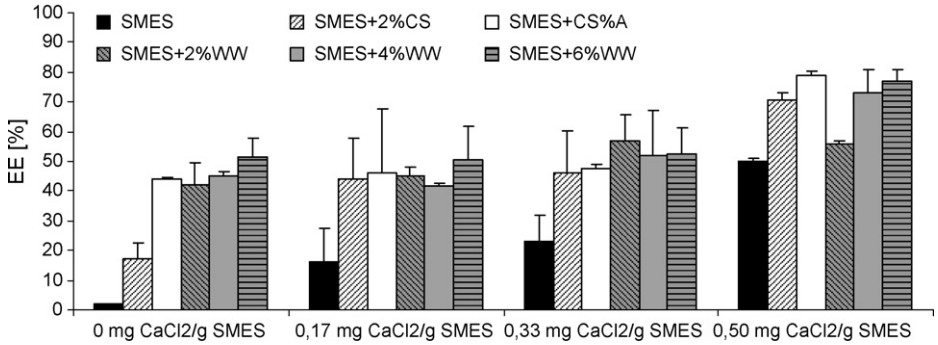

Fig. 5. Influence of $CaCl_2$ concentration in SMES and concentration of thickening agents (colloidal silica (CS), white wax (WW)) on encapsulation efficiency (EE) of furosemide-loaded SMES.

process complexity by thermostating the system at low temperature, suitable thickening agents were added to SMES that can modify its rheological behaviour without significant influence on other features of the (micro)emulsions (Špiclin et al., 2003; Rozman et al., 2009).

The density of the core forming phase was also influenced by thickening SMES with colloidal silica or white wax (Table 2). Though, while addition of colloidal silica increased the density of the SMES, the opposite effect was observed when 4–6% (w/w) of white wax was added. The densities of the shell and core forming phases should be alike when producing microcapsules by the vibrating nozzle method. In agreement with this, higher furosemide encapsulation efficiency was achieved when SMES was thickened with 2% (w/w) white wax (~42%) instead of colloidal silica (~17%). Yet, comparable results were obtained for SMES containing 4–6% (w/w) of the two thickening agents (Table 2), even though the difference in core density is even more pronounced in this case and therefore even more distinctive influence on encapsulation efficiency could be expected. This suggests that the microencapsulation process is more affected by core phase viscosity than core phase/shell phase density ratio.

Yet, a complementary effect was observed when merging both approaches discussed above. The highest encapsulation (70–80%) was thus obtained when SMES containing 0.5 mg $CaCl_2$/g SMES and thickened with 4–6% (w/w) colloidal silica or white wax was used as the core phase (Fig. 5, last group of columns). As shown in Fig. 5 (second group of columns), addition of 0.17 mg $CaCl_2$/g SMES resulted in increased encapsulation only for unthickened SMES and for SMES containing 2% (w/w) colloidal silica. When $CaCl_2$ was added at higher amounts (0.33 or 0.55 mg $CaCl_2$/g SMES), increased encapsulation was observed for all systems used as core forming phase.

3.3.2. Drying of microcapsules

After incubation in the hardening solution, microcapsules appeared smooth and spherical, with distinct core and shell. Microcapsules with optimal core composition (SMES with 4% colloidal silica and SMES with 4% white wax, w/w) were dried by different procedures and characterized for furosemide encapsulation (Fig. 6) and visual appearance (Fig. 7). Only a slight decrease in furosemide content was observed when microcapsules were dried in a fluid bed system, whereas freeze-drying and drying in air caused core phase leakage, with large decreases in furosemide encapsulation (Fig. 6). This decrease may be related to the time of drying, being the shortest when using the fluid bed system. Irrespective of the technique applied, drying resulted in microcapsules that are not perfect spherical and have a rough surface due to shrinking of the pectin gel. In keeping with the observed core phase leakage, the modification of microcapsule size and shape was the most distinct when they were allowed to dry in air. Shrinking was the least pronounced when microcapsules were freeze-dried, nevertheless their structure was too porous to retain the liquid core. On the basis of these results, drying in the fluid bed system was selected as the optimal drying method, the furosemide retention being the highest and the microcapsules being well shaped.

Table 2
The density (ρ) and encapsulation efficiency (EE) of unthickened and thickened SMES.

	ρ (g cm^{-3})	EE (%)
SMES	1.0429 ± 0.0003	2 ± 0.52
SMES + 2%CS	1.0557 ± 0.0003	16.98 ± 5.51
SMES + 4%CS	1.0661 ± 0.0002	43.99 ± 0.72
SMES + 6%CS	–	–
SMES + 2%WW	1.0430 ± 0.0006	42.21 ± 7.32
SMES + 4%WW	1.0416 ± 0.0009	45.05 ± 1.39
SMES + 6%WW	1.0408 ± 0.0007	51.55 ± 6.09
shell-forming phase	1.0253 ± 0.0002	–

3.4. Drug release studies

The influence of self-microemulsifying core on drug release is shown in Fig. 8, where dissolution profiles of the microcapsules with self-microemulsifying cores of different composition are compared with the reference microspheres (without core). In vitro release experiments were conducted in hydrochloric acid solution, pH 3, (Fig. 8a) and phosphate buffer, pH 6.8 (Fig. 8b).

Drug release at pH 6.8 was faster than at pH 3. At pH 6.8, drug release was fairly rapid with essentially complete release within 2–3 h, and after 4 h the microcapsules as well as the microspheres

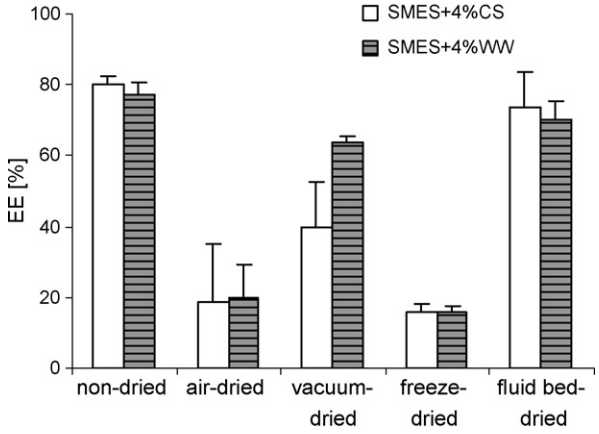

Fig. 6. The effect of different drying procedures on furosemide encapsulation efficiency (EE), compared to non-dried microcapsules.

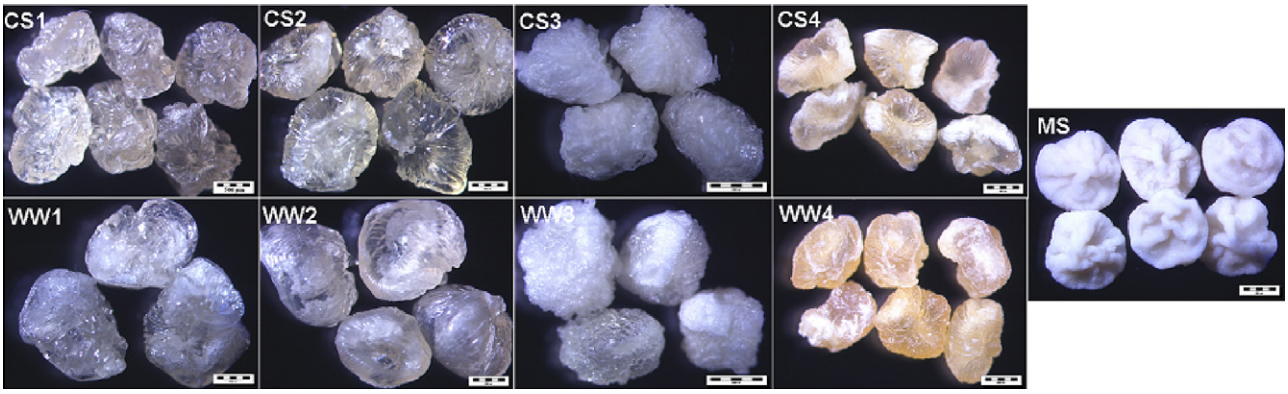

Fig. 7. Microcapsules with self-microemulsifying core, thickened with colloidal silica (CS) or white wax (WW), after drying in the fluid bed system (CS1, WW1) vacuum (CS2, WW2), freeze-drying (CS3, WW3) and in air (CS4, WW4). Reference microspheres without SMES in the core, dried in fluid bed system, are also presented (MS). Size bars represent 500 μm.

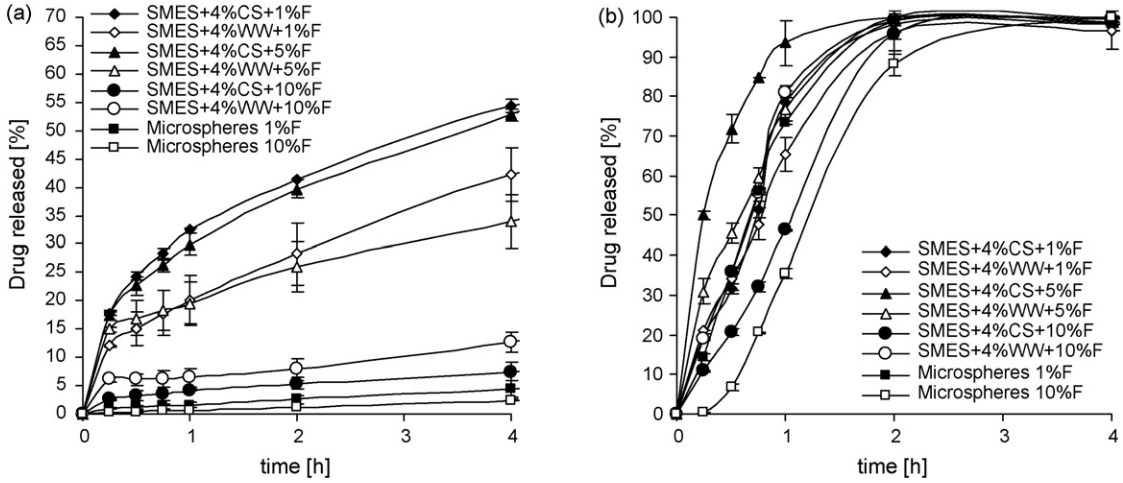

Fig. 8. Percentage of furosemide released from microcapsules with a self-microemulsifying core (thickened with 4% colloidal silica (CS) or white wax (WW) and containing 1–10% furosemide) or reference microspheres (without self-microemulsifying core) loaded with 1 or 10% furosemide in (a) aqueous HCl at pH 3 and (b) phosphate buffer, pH 6.8; $n = 3$.

were disintegrated. Furosemide release was slower at pH 3, where microcapsules and microspheres retained their structure throughout the experiment. Furthermore, furosemide ($pK_a \sim 3.9$) at pH 3 exists mainly in its unionized form that is poorly water soluble whereas at pH 6.8 it is ionized and therefore better water soluble. Since the effect of self-microemulsifying core on drug release profile can be better observed at pH 3, these results were used to provide more detailed interpretation of release properties.

Microspheres and microcapsules with self-microemulsifying core showed great differences in in vitro release profiles. Microcapsules released up to 55% of furosemide in 4 h, whereas microspheres released less than 5%. This is in agreement with the ability of SMES to avoid the drug dissolution step in the gastrointestinal tract by delivering drugs in dissolved form (Neslihan and Benita, 2004; Porter et al., 2007).

The drug release profile was also influenced by adding thickening agent to the self-microemulsifying core (Fig. 8a). Furosemide release was faster from microcapsules containing colloidal silica in the core phase (up to ~55% of drug released in 4 h) than from those thickened with white wax (up to ~42% of drug released in 4 h). This can be explained by the higher hydrophobicity of white wax that slows down the self-emulsification process and, consequently, drug release.

Drug release was also dependent on the concentration of furosemide in SMES. As expected, self-microemulsifying cores with completely solubilized drug (SMES with 1 and 5% furosemide) exhibited the fastest release profiles with pronounced initial release (Fig. 8a). In the case of self-microemulsifying cores with 10% furosemide the maximum solubility of furosemide was exceeded and part of the furosemide was suspended in SMES, so the release was limited by dissolution of the suspended drug.

4. Conclusions

Production of Ca-pectinate microcapsules with self-microemulsifying core by vibrating nozzle method was successfully modified to allow encapsulation of SMES with high efficiency. Moreover, SMES composed of 12% (w/w) oil phase and 88% (w/w) surfactant mixture enabled solubilization of furosemide in high concentration (86 mg/ml SMES). The efficiency of its encapsulation within the pectinate matrix was high when 0.5 mg $CaCl_2$/g SMES was added to the core phase, thickened with 4–6% (w/w) colloidal silica or white wax, and with subsequent drying of the microcapsules in the fluid bed system. Furthermore, the permeability of furosemide was enhanced by its implementing into SMES; most probably by altering apical membrane fluidity, opening tight junctions and inhibiting efflux transporters involved in the intestinal secretion of furosemide. Also the dissolution rate of furosemide from microcapsules was considerably faster than from reference microspheres (without a self-microemulsifying

core). Better solubility and permeability properties obtained with SMES, as shown in this paper, could thus provide a promising alternative to ensure successful oral delivery of drugs with poor biopharmaceutical properties.

Acknowledgements

Authors would like to thank Prof. Roger H. Pain for proof reading the manuscript. We acknowledge assistant Dr. Simon Žakelj for his help with HPLC analysis.

References

Abdalla, A., Klein, S., Mäder, K., 2008. A new self-emulsifying drug delivery system (SEDDS) for poorly soluble drugs: characterization, dissolution, in vitro digestion and incorporation into solid pellets. Eur. J. Pharm. Sci. 35, 457–464.

Berginc, K., Žakelj, S., Levstik, L., Uršič, D., Kristl, A., 2007. Fluroscein transport properties across artificial membranes. Caco-2 cells monolayer and rat jejunum. Eur. J. Pharm. Biopharm. 2, 281–285.

Beyers, H., Malan, S.F., van der Watt, J.G., de Villiers, M.M., 2000. Structure–solubility relationship and thermal decomposition of furosemide. Drug Dev. Ind. Pharm. 26, 1077–1083.

Burcham, D.I., Maurin, M.B., Hausner, E.A., Huang, S.M., 1997. Improved oral bioavailability of the hypocholestrolemic DMP 565 in dogs following oral dosing in oil and glycol solutions. Biopharm. Drug Dispos. 18, 737–742.

Chiou, W.L., Barve, A., 1998. Linear correlation of the fraction of oral dose absorbed of drugs between humans and rats. Pharm. Res. 11, 1792–1795.

Constantinides, P.P., 1995. Lipid microemulsions for improving drug dissolution and oral absorption: physical and biopharmaceutical aspects. Pharm. Res. 12, 1561–1572.

Constantinides, P.P., Wasan, K.M., 2007. Lipid formulation strategies for enhancing intestinal transport and absorption of P-glycoprotein (P-gp) substrate drugs: in vitro/in vivo case studies. J. Pharm. Sci. 96, 235–248.

Daham, A., Hoffman, A., 2007. The effect of different lipid based formulations on the oral absorption of lipophilic drugs: the ability of in vitro lipolysis and consecutive ex vivo intestinal permeability data to predict in vivo bioavailability in rats. Eur. J. Pharm. Biopharm. 67, 96–105.

Homar, M., Šuligoj, D., Gašperlin, M., 2007. Preparation of microcapsules with self-microemulsifying core by a vibrating nozzle method. J. Microencapsul. 24, 72–81.

Jannin, V., Musakhanian, J., Marchaud, D., 2007. Approaches for the development of solid and semi-solid lipid-based formulations. Adv. Drug Deliv. Rev. 60, 734–746.

Jumaa, M., Furkert, F.H., Muller, B.W., 2002. A new lipid emulsion formulation with high antimicrobial efficacy using chitosan. Eur. J. Pharm. Biopharm. 53, 115–123.

Lee, M.G., Chiou, W.L., 1983. Evaluation of potential causes for the incomplete bioavailability of furosemide: gastric first-pass metabolism. J. Pharmacokinet. Biopharm. 11, 623–640.

Maclean, C., Moenning, U., Reichel, A., Fricker, G., 2008. Closing the gaps—a full scan of the intestinal expression of Pgp. Bcrp and Mrp2 in male and female rats. Drug Metab. Dispos. 36, 1249–1254.

Nazzal, S., Khan, M.A., 2006. Controlled drug release of a self-emulsifying formulation from a tablet dosage form: stability assessment and optimization of some processing parameters. Int. J. Pharm. 315, 110–121.

Neslihan, G.R., Benita, S., 2004. Self-emulsifying drug delivery systems (SEDDS) for improved oral delivery of lipophilic drugs. Biomed. Pharmacother. 58, 173–182.

Patil, P., Patil, V., Paradkar, A., 2007. Formulation of self emulsifying system for oral delivery of simvastatin: in vitro and in vivo evaluation. Acta Pharm. 57, 111–122.

Porter, C.J.H., Trevaskis, N.L., Charman, W.N., 2007. Lipids and lipid-based formulations: optimizing the oral delivery of lipophilic drugs. Nat. Rev. Drug Discov. 6, 231–248.

Pouton, C.W., 2000. Lipid formulations for oral administration of drugs: non-emulsifying, and 'self-microemulsifying' drug delivery systems. Eur. J. Pharm. Sci. 11, S93–S98.

Rege, B., Kao, J., Polli, J., 2002. Effect of non-ionic surfactants on membrane transports in Caco-2 cell monolayers. J. Pharm. Sci. 16, 237–246.

Rozman, B., Gašperlin, M., Tinois-Tessoneaud, E., Pirot, F., Falson, F., 2009. Simultaneous absorption of vitamins C and E from topical microemulsions using reconstructed human epidermis as a skin model. Eur. J. Pharm. Biopharm. 72, 69–75.

Serratoni, M., Newton, M., Booth, A., Clarke, A., 2007. Controlled drug release from pellets containing water-insoluble drugs dissolved in a self-emulsifying system. Eur. J. Pharm. Biopharm. 65, 94–98.

Shah, N.H., Carvajal, M.T., Patel, C.I., 1994. Self-emulsifying drug delivery systems (SEDDS) with polyglycolyzed glycerides for improving in vitro dissolution and oral absorption of lipophilic drugs. Int. J. Pharm. 106, 15–23.

Shawn, D., Flanagan, S.D., Benet, L.Z., 1999. Net secretion of furosemide in subject to indomethacin inhibition, as observed in Caco-2 monolayers and excitsed rat. Pharm. Res. 2, 221–224.

Siissalo, S., Hannikainen, J., Kolehmainen, J., Hirvonen, J., Kaukonen, A.M., 2009. A Caco-2 cell based screening method for compounds interaction with MRP2 efflux protein. Eur. J. Pharm. Biopharm. 71, 332–338.

Šentjurc, M., Vrhovnik, K., Kristl, J., 1999. Liposomes as a topical delivery system: the role of size on transport by the EPR imaging method. J. Control. Release 1, 87–97.

Špiclin, P., Homar, M., Zupančič-Valant, A., Gašperlin, M., 2003. Sodium ascorbyl phosphate in topical microemulsions. Int. J. Pharm. 256, 65–73.

Tan, A., Simovic, S., Davey, A.K., Rades, T., Prestidge, C.A., 2009. Silica-lipid hybrid (SLH) microcapsules: a novel oral delivery system for poorly soluble drugs. J. Control. Release 134, 62–70.

Wandel, C., Kim, R.B., Stein, M., 2003. "Inactive" excipients such as Cremophor can affect in vivo drug disposition. Clin. Pharmacol. Ther. 73, 394–396.

Xianyi, S., Guijun, Y., Yunjuan, W., Junchan, L., Xiaoling, F., 2005. Effect of self-emulsifying drug delivery systems containing Labrasol on tight junctions in Caco-2 cells. Eur. J. Pharm. Sci. 24, 477–486.

Zvonar, A., Rozman, B., Bešter Rogač, M., Gašperlin, M., 2009. The influence of microstructure on celecoxib release from a pharmaceutically applicable system: Mygliol 812®/Labrasol®/Plurol oleiquer®/water mixtures. Acta Chim. Slov. 56, 131–138.